2010 IEEE International Conference on Robotics and Automation
Anchorage Convention District
May 3-8, 2010, Anchorage, Alaska, USA

Frequency Criteria for the Grasping Control of a Hyper-redundant Robot

Mircea Ivanescu, *Member, IEEE*, Nicu Bizdoaca, Mihaela Florescu, Nirvana Popescu, Decebal Popescu

Abstract— **The paper focuses on hyper-redundant arms with continuum elements that perform the grasping function by coiling. First, there is concern with the dynamic model of the continuum arm for the position control during non-contact operations with the environment. A frequency stability criterion based on the Kahman – Yakubovich – Popov Lemma and P and PD control algorithms is proposed. Then, the grasping control of the arm in contact with a load is analyzed. The dynamics of the system are discussed and an extension of the Popov criterion is endorsed. The control algorithms based on SMA actuators are introduced. Numerical simulations and experimental results of the arm motion toward an imposed target are presented.**

I. Introduction

The hyper-redundant arms with continuum elements are a special class of robots that perform the grasping function by coiling. This function is often met in the animal world. The elephant trunk, the octopus tentacle or constrictor snakes represent the well-known biological models. The enveloping grasps are superior in terms of restraining objects. As a technical solution, the grasping by wrapping, by coiling is used for restraint, fixturing and dexterous manipulation.

The control of these systems is complex, indeed, and a large number of researchers have tried to cater solutions. In [2], Gravagne analyzed the kinematic model of "hyper-redundant" robots, known as "continuum" robots. Remarkable results were achieved by Chirikjian and Burdick [6], who laid the foundations of the kinematic theory of hyper-redundant robots. Their findings are based on a "backbone curve" that captures the robot's macroscopic geometric features. Mochiyama investigated the problem of controlling the shape of an HDOF rigid-link robot with two-degree-of-freedom joints using spatial curves [7]. In [8], the "state of art" of continuum robots, their areas of application and some control issues are presented. Other papers [9, 10] deal with several technological solutions for actuators used in hyper-redundant structures and with conventional control systems.

The current paper investigates the control problem of a class of hyper-redundant arms with continuum elements that performs the grasping function by coiling. The dynamics of the arm during non-contact or contact operations with the environment are analyzed. The frequency criteria for the stability and control algorithms are also discussed. The paper is organized as follows: Section II presents technological and theoretical preliminaries; Section III studies the dynamic model for non-contact motions; Section IV presents a frequency criterion and position control law; Section V discusses the dynamics of the arm and load in a grasping function; Section VI presents an extension of the Popov criterion for this class of systems; Section VII verifies the control laws by computer simulation; Section VIII presents some experimental results.

II. Technological and Theoretical Preliminaries

The hyper-redundant technological models are complex structures that operate in 3D space, but the grasping function of these arms is, generally, a planar function. Accordingly, the model discussed in this paper is a 2D model.

The technological model basis is presented in Fig.1.a. It consists of layered structures that ensure the flexibility, driving and position measuring. The high flexibility is obtained by an elastic backbone rod.

The driving layer is made up of two antagonistic SMA actuators, A and B, each of them having a number of SMA fibers that are connected to the ends of the beam and determine its bending by current control. These SMA fibers are well suited for grasping force control due to their high strength to weight ratio.

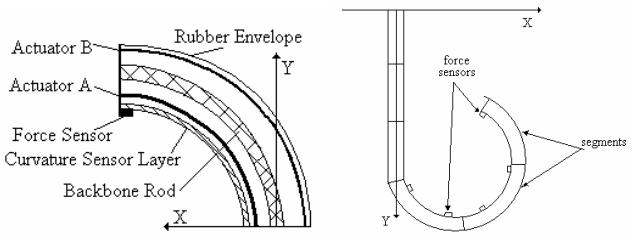

(a) (b)

Fig.1. (a) The segment layer structure; (b) The arm structure

The measuring layer is represented by an electro-active polymer curvature sensor. This sensor is placed on the boundary of the beam and allows for its curvature measuring by the resistance measuring. The sensor system is completed by a number of force sensors placed at each terminal of the beam segment. A rubber envelope protects and isolates this layer structure from the operator environment.

The general form of the arm is shown in Fig.1.b. It consists of a number (N) of segments and the last m segments $(m < N)$ represent the grasping terminals.

As a theoretical model, we shall consider the beam in Fig.2.a with the length L and the thickness l. This beam has been deflected into a circular arc by a SMA fiber. The beam is composed of concentric arcs. The neutral arc defines the curvature of the beam,

$$c_V = \frac{d\phi}{ds},\ \phi = \frac{s}{R_c} \tag{2.1}$$

where ϕ represents the angle of the current position, s is the arc length from the origin, and R_c is the radix of the arc.

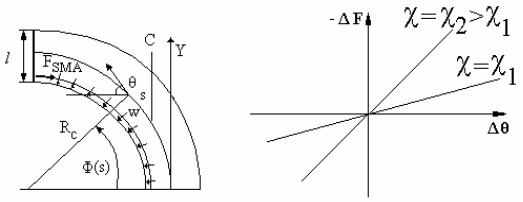

(a) (b)

Fig.2. (a) The arm parameters; (b) The force variation

We denote the equivalent force developed by the SMA actuators at the end of the beam $(s = L)$ by χ, the force density and the distributed force along the beam exercised by the SMA fibers on the beam surface by w and F, respectively, and τ is the equivalent moment of the beam.

From [11], we have the following relations

$$w = \frac{dF}{ds},\ w = \chi \cdot c_V,\ \tau = \chi \cdot \frac{l}{2} \tag{2.2}$$

$$dF = \chi \cdot d\phi,\ dF = -\chi \cdot d\theta \tag{2.3}$$

This relation allows us to estimate the variations of the force on the beam surface as a function of the angle coordinate variations for a specified force χ exercised by the actuators. These relations are shown in Fig.2.b.

Fig.2.a illustrates the backbone of the beam represented by the curve C. We can use a parameterization of the curve C based upon a continuous angle $\theta(s)$,

The position of a point s on the curve C is defined by the position vector $r = r(s)$, $s \in [0, L]$. For a dynamic motion, the time variable will be introduced, $r = r(s,t)$,

$$r(s,t) = \begin{bmatrix} x(s,t) & y(s,t) \end{bmatrix}^T \tag{2.4}$$

The beam has the elastic modulus E_b, the moment of inertia I_b, the bending stiffness $E_b I_b$, the linear mass density ρ_b and rotational inertial density I_{b_ρ}.

I. Dynamic Model

The dynamic model of the arm can be derived by using the Hamilton principle [7],

$$\delta \int_0^t \left(T_k - V_p + W_v + W_f + L_f \right) dt = 0 \tag{3.1}$$

where T_k is the kinetic energy, V_p is the potential elastic energy (the gravitational potential energy is neglected for this light-weight arm), W_f and L_f are the work energies of the applied external forces and W_v is the viscous damping work.

Using the same procedure as in [5], we have the partial differential equations of the arm

$$I_{\rho b}\ddot{\theta}_b + b_b\dot{\theta}_b - E_b I_b \frac{\partial^2 \theta}{\partial s^2} + c_b F = 0 \tag{3.2}$$

with the initial and boundary conditions

$$\theta_b(0,s) = \theta_{b0}(s);\ \dot{\theta}(0,s) = 0 \tag{3.3}$$

$$E_b I_b \cdot \frac{\partial \theta_b(t,L)}{\partial s} = \tau_L;\qquad \frac{\partial \theta_b(t,0)}{\partial s} = 0;\qquad \frac{\partial \dot{\theta}_b(t,0)}{\partial s} = 0;$$

$$\frac{\partial \dot{\theta}_b(t,L)}{\partial s} = -\alpha_1 \theta_b(t,L) - \alpha_2 \dot{\theta}_b(t,L) \tag{3.4}$$

where $\theta_b = \theta_b(t,s)$, $\dot{\theta}_b$ represents $\frac{\partial \theta_b(t,s)}{\partial t}$, b_b is the equivalent damping coefficient of the beam, α_1, α_2 are the coefficients that determine the constraints on the boundary, $\alpha_1 \geq 0$, $\alpha_2 > 1$, and τ_L is the actuator input torque generated at the beam boundary $s = L$. From (2.2), it results that

$$\tau_L(t) = \tau(L,t) = \frac{l}{2} \cdot \chi \tag{3.5}$$

We consider that the initial and desired states of the system are given by the curves C_0, C_d, respectively,

$$C_0 : (\theta_{b0}(s)),\ C_d : (\theta_{bd}(s)),\ s \in [0, L] \tag{3.6}$$

We define by $e_b(t,s)$ the position error,

$$e_b(t,s) = \Delta\theta(t,s) = \theta_b(t,s) - \theta_{bd}(s) \tag{3.7}$$

In terms of the error, the dynamic model (3.2) – (3.4) can be rewritten as

$$I_{\rho b}\ddot{e}_b + b_b\dot{e}_b - E_b I_b \frac{\partial^2 e_b}{\partial s^2} + c_b f = 0 \tag{3.8}$$

$$E_b I_b \cdot \frac{\partial e_b(t,s)}{\partial s} = \tau^* \tag{3.9}$$

when f , τ^* are determined by the relations

$$f = f(t,s) = F(t,s) - F_d(s),\ \tau^* = \tau^*(t) = \tau(t) - \tau_d \quad (3.10)$$

and F_d , τ_d are the static backbone force and moment, respectively, applied by the actuators,

$$-E_b I_b \cdot \frac{\partial^2 \theta_d}{\partial s^2} = F_d\ ,\ E_b I_b \cdot \frac{\partial \theta_d(L)}{\partial s} = \tau_d \quad (3.11)$$

The equation (3.2) can be rewritten in a matrix form,

$$\dot{e} = A\frac{\partial^2 e}{\partial s^2} + Be + cf \quad (3.12)$$

with initial and boundary conditions

$$e(0,x) = e_0(x)\ ;\ e(t,0) = 0\ ;\ \frac{\partial e(t,0)}{\partial s} = 0 \quad (3.13)$$

$$E_b I_b \frac{\partial e_b(t,L)}{\partial s} = \tau^* \quad (3.14)$$

$$\frac{\partial \dot{e}_b(t,0)}{\partial s} = 0\ ;\ \frac{\partial \dot{e}_b(t,L)}{\partial s} = -\alpha_1 e_b(t,L) - \alpha_2 \dot{e}_b(t,L) \quad (3.15)$$

where $e = \left[e_b,\quad \dot{e}_b\right]^T$ (3.16)

$$A = \begin{bmatrix} 0 & 0 \\ \dfrac{E_b I_b}{I_{b\rho}} & 0 \end{bmatrix};\ B = \begin{bmatrix} 0 & 1 \\ 0 & -\dfrac{b_b}{I_{b\rho}} \end{bmatrix} \quad (3.17)$$

$$c = \begin{bmatrix} 0 & -\dfrac{c_b}{I_{b\rho}} \end{bmatrix}^T\ ;\ d = \left[E_b I_b \quad 0\right]^T \quad (3.18)$$

II. Main results (1)

The closed loop system of the arm is represented in Fig.3. The dynamic model is defined by equations (3.12) – (3.18), and the control force $f = \Delta F$ is generated by a linear variation of the angle error $\Delta\theta$ with the gradient χ . The magnitude χ is produced by the SMA fibers at the end of the beam.

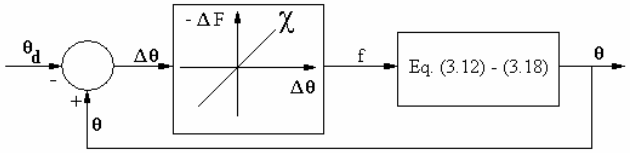

Fig.3. The control position closed loop system

Theorem 1. The closed loop system (Fig.3) is absolutely stable if:

(1) $(-A+B)$ is a Hurwitzian matrix;

(2) the pair $(-A+B, C)$ is completely controllable;

(3) there is a positive definite and symmetrical matrix P such that $\left(A^T P + PA\right)$ is positive definite;

$$(4)\ \frac{1}{\chi} + \mathrm{Re}\left[n^T\left(j\omega I - (-A+B)\right)^{-1} c\right] \geq 0 \quad (4.1)$$

(5) the moment control law is

$$\tau^*(t) = -k_p e_b(t,L) - k_d \dot{e}_b(t,L) \quad (4.2)$$

where the coefficients k_p , k_d are chosen so as to the matrix

$K = \begin{bmatrix} \dfrac{k_p}{E_b I_b} - 1 & \dfrac{k_d}{E_b I_b} \\ \alpha_1 & \alpha_2 - 1 \end{bmatrix}$ will be positive definite.

Proof. See Appendix 1.

Remark 1. The condition (1) – (3) are easily verified for a beam with normal elastic properties. Condition (4) allows us to introduce a frequency criterion. If we denote this condition by

$$G(j\omega) = n^T\left(j\omega I - (-A+B)\right)^{-1} c \quad (4.4)$$

it can be easily graphically interpreted. Let $\tilde{G}$ be the plot of $G(j\omega)$ in the $G(j\omega)$-plane. Condition (4) requires that the plot $\tilde{G}$ cross the negative real axis at a point that lies to the right of the critical point defined by $-\dfrac{1}{\chi}$ (Fig.4).

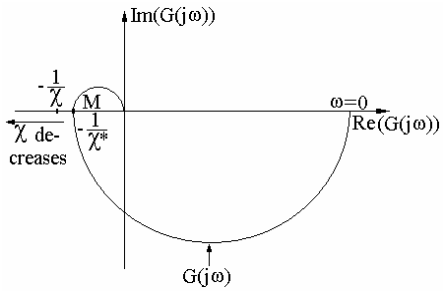

Fig.4. The plot of $G(j\omega)$ for the position control

Let *M* be the point of intersection of $\tilde{G}$ with the real axis. This point defines the limit value of $\chi = \chi^*$ that ensures the stability of the motion for a specified beam.

Remark 2. Condition (5) implies a PD boundary controller in the actuation system, but the derivative control component is difficult to be implemented by SMA actuators.

A P control component is preferable; the condition (4.2) becomes

$$\tau^*(t) = -k_p e_b(t,L), \quad k_p > E_b I_b \tag{4.5}$$

From (2.3) and (4.5) it results

$$|\chi| = \frac{2k_p|e_b|}{l} = \frac{2k_p|\Delta\theta(t,L)|}{l} \le \chi^* \tag{4.6}$$

The upper limit of k_p can be obtained for the maximum value of $\Delta\theta(t,L)$, which can be evaluated by the curvature resistive sensor, $\Delta\theta = k_R(R_d - R_0) = k_R\Delta R$, where k_R is a sensor proportionality coefficient, assumed to be constant for the domain of motion, and R_d, R_0 are the sensor resistances at the desired and initial position, respectively.

The lower limit of k_p is defined by the positiveness condition (4.5).

$$E_b I_b < k_p \le \frac{\chi^* l}{2k_R \cdot \Delta R} \tag{4.7}$$

Remark 3. The tension χ is generated by the pair of antagonistic SMA actuators (Fig.1), each actuator consisting of *N* parallel fibers. Theoretical modeling and open loop experiments have shown that the antagonistic force response of the SMA actuators behaves like an integrator while the input current is applied. A current pulse-width modulated controller, in which the control variable is the duration of the input signal at constant current amplitude, is used [13].

The average value of the force can be evaluated as

$$F_{SMA}^{med} = \lambda \cdot (I^*)^2 \cdot \frac{T_D^2}{T_p}, \quad \lambda = \frac{a_f N R_f}{2c_g} \tag{4.8}$$

where T_p is the wave period, I^* is the current amplitude, T_D is the pulse duration, *N* is the number of fibers, a_f – the fiber cross sectional area, R_f – the fiber resistance, and c_g is the material complex coefficient defined by the specific heat, latent heat, stress rate, austenite and finish temperatures and mass of the fiber.

Considering $|\chi| \approx F_{SMA}^{med}$, and using the P control (4.5), we have

$$T_D = \alpha\left(|e_b(t,L)|\right)^{1/2}, \quad \alpha = \frac{1}{I^*}\cdot\left(\frac{2k_P T_P}{\lambda l}\right)^{1/2} \tag{4.9}$$

A simpler control law of T_D can be obtained if the wave generator ensures a constant ratio $\frac{T_D}{T_P} = \beta$. In this case, the control algorithm of T_D becomes

$$T_D = \alpha^* \cdot |e_b(t,L)|, \quad \alpha^* = \frac{2k_P}{(I^*)^2 \cdot \lambda\beta l} \tag{4.10}$$

Besides, the force inequality (4.6) can be expressed in terms of the limit of the current pulse duration T_D^*,

$$T_D^* \le \frac{1}{(I^*)^2 \cdot \lambda\beta} \cdot \chi^* \tag{4.11}$$

III. GRASPING DYNAMIC MODEL

The grasping function control is represented by the force control between the arm and load. Consider that the arm has achieved the desired position defined by the surface (object).

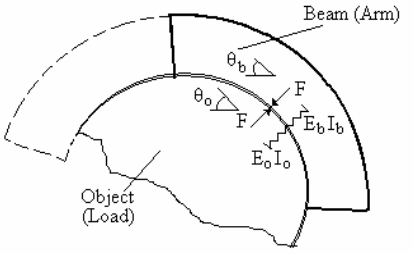

Fig.5. The grasping model

In Fig.5, an object with elastic and damping parameters $E_o I_o$, b_o and c_o, respectively, is grasped by coiling. Using the same procedure as developed in Section 3, the dynamic model of the two bodies in contact, arm and load, is represented by the following partial differential equations,

$$\dot{\tilde{e}} = \tilde{A}\frac{\partial^2 \tilde{e}}{\partial s^2} + \tilde{B}\tilde{e} + \tilde{c}f \tag{5.1}$$

$$\tilde{e}(0,s) = 0;\ \tilde{e}(t,0) = \frac{\partial \tilde{e}(t,0)}{\partial s} = 0 \tag{5.2}$$

$$E_b I_b \cdot \frac{\partial e_b(t,L)}{\partial s} = \tau^* \tag{5.3}$$

$$e_b(t,L) = e_\theta(t,L);\ \frac{\partial e_o(t,L)}{\partial s} = \frac{\partial e_b(t,L)}{\partial s} \tag{5.4}$$

$$\frac{\partial \dot{\tilde{e}}(t,L)}{\partial s} = -\alpha_1 \tilde{e}(t,L) - \alpha_2 \dot{\tilde{e}}(t,L) \tag{5.5}$$

where $\tilde{e}(t,s)=\left[e_b(t,s),\quad e_o(t,s)\right]^T$, with $e_b(t,s)=\theta_b(s)-\theta_{bd}(s)$; $e_o(t,s)=\theta_o(s)-\theta_{od}(s)$, f is the force error, τ^* is the control variation, defined as in (3.10), and the indices *b* and *o* specify the parameters of the beam and object, respectively.

$$\tilde{A}=\begin{bmatrix} 0 & 0 & 0 & 0 \\ \frac{1}{I_{\rho b}}\left(E_bI_b+E_oI_o\right) & 0 & -\frac{E_oI_o}{I_{\rho b}} & 0 \\ 0 & 0 & 0 & 0 \\ -\frac{E_oI_o}{I_{\rho o}} & 0 & \frac{E_oI_o}{I_{\rho o}} & 0 \end{bmatrix} \tag{5.6}$$

$$\tilde{B}=\begin{bmatrix} 0 & 1 & 0 & 0 \\ 0 & -\frac{b_b}{I_{\rho b}} & 0 & 0 \\ 0 & 0 & 0 & 1 \\ 0 & 0 & 0 & -\frac{b_b}{I_{\rho o}} \end{bmatrix};\qquad \tilde{c}=\begin{bmatrix} 0 \\ \frac{c_b}{I_{\rho b}} \\ 0 \\ -\frac{c_o}{I_{\rho o}} \end{bmatrix} \tag{5.7}$$

IV. Main results (2)

The grasping force control is the second problem of the grasping control. A force sensor network is used to account for the contact between the arm and the load. We notice, from (2.2), that the force density *w* is constant along the arm segment and, in a steady state, *w* can be approximated to *f*. A force sensor with the position $s=s^*\in[0,L]$ is used to measure the contact force. The contact force – displacement relation of the sensor is assumed to lie in the positive sector (Fig.6).

$$\Delta F=-\psi(\Delta\theta),\ \psi(\Delta\theta)\cdot\Delta\theta\ge 0 \tag{6.1}$$

$$\psi(0)=0\ \text{ for }\ \Delta\theta=0 \tag{6.2}$$

The nonlinearity $\psi(\Delta\theta)$ is single-valued, time invariant and constraint to a sector bounded by slope k_s which is assumed to meet

$$0\le\frac{\psi(\Delta\theta)}{\Delta\theta}\le k_s<\infty \tag{6.3}$$

which is the case for most physically realistic elastic contacts.

In terms of the sensor characteristics, the convergence to zero of the error e_b is equivalent to the convergence to zero of the contact force error *f*

$$\lim_{t\to\infty}e_b\left(t,s^*\right)=0\ \Rightarrow\ \lim_{t\to\infty}f\left(t,s^*\right)=0 \tag{6.4}$$

The sensor nonlinearity (6.1) – (6.3) and the dynamic model of the grasping contact described by (5.1) – (5.5) suggest the closed – loop system of Fig.6.

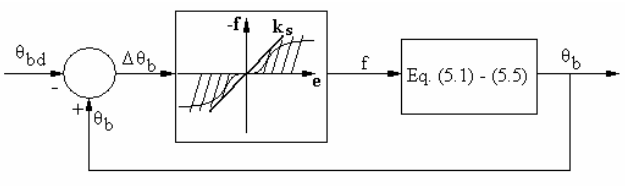

Fig.6. The grasping control closed loop system

Theorem 2. The closed – loop system (Fig.6) is absolutely stable if:

(1) $\left(-\tilde{A}+\tilde{B}\right)$ is a Hurwitzian matrix;

(2) the pair $\left(-\tilde{A}+\tilde{B},\quad \tilde{c}\right)$ is completely controllable;

(3) there is a positive definite and symmetrical matrix *P* such that $\left(\tilde{A}^TP+P\tilde{A}\right)$ is positive definite;

(4) $$\frac{1}{k_s}+\mathrm{Re}\left[\tilde{n}^T\left(j\omega I-\left(-\tilde{A}+\tilde{B}\right)\right)^{-1}\tilde{c}\right]\ge 0 \tag{6.5}$$

(5) the moment of the arm verifies the relation

$$\tau^*=k_pe_b(t,L),\qquad k_p>E_bI_b \tag{6.6}$$

Proof. See Appendix 2.

Equations (6.1), (6.3) and (5.1) – (5.5) describe the closed loop system (Fig.6), consisting of a partial derivative equation linear system and a nonlinear element represented by the function $\psi(\cdot)$ belonging to the sector $[0,k_s]$. In this case, the condition (4) represents the Popov criterion for this class of systems. According to it, the system will be absolutely stable if the plot of $\tilde{G}(j\omega)$

$$\tilde{G}(j\omega)=\tilde{n}^T\left[j\omega I-\left(-\tilde{A}+\tilde{B}\right)\right]^{-1}\tilde{c} \tag{6.7}$$

crosses the negative real axis at a point that lies to the right of the critical point defined by $-\frac{1}{k_s}$ (Fig.7).

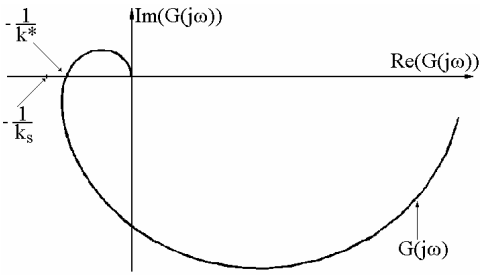

Fig.7. The plot of $G(j\omega)$ for the grasping control

For a pair "arm – load" specified, the plot of $\tilde{G}(j\omega)$ has a well-defined characteristic and the intersection with the real axis determines the limit value of k. Let k^* be the corresponding value of the crossing point. The absolute stability is guaranteed if the sensor parameters meet the condition

$$k_s \le k^* \tag{6.8}$$

V. Simulation

A hyper-redundant manipulator with 4 segments is considered. The parameters of the arm were selected run as follows: bending stiffness $E_b I_b = 1$, linear mass density $\rho_b = 0.5\,kg/m$, rotational inertial density $I_{\rho b} = 0.001 kg \cdot m^2$ and damping ratio 0.35. These constants are realistic for long thin backbone structures. The grasping function is exercised by the last three segments of the arm, the length of each arm segment is $L = 1$ (Geometrical parameters are scaled.). The load is a cylinder with the radix $R = 1$, bending stiffness $E_o I_o = 0.2$, rotational inertial density and damping ratio 0.22.

Fig.8 illustrates the grasping function of the arm. The initial position is a vertical one, and the arm motion by coiling of the arm can be seen.

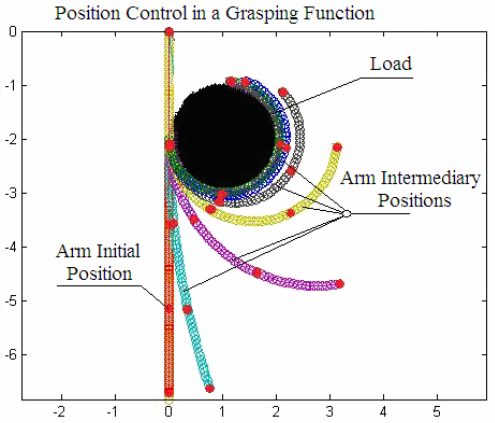

Fig.8. The simulation of the grasping operation

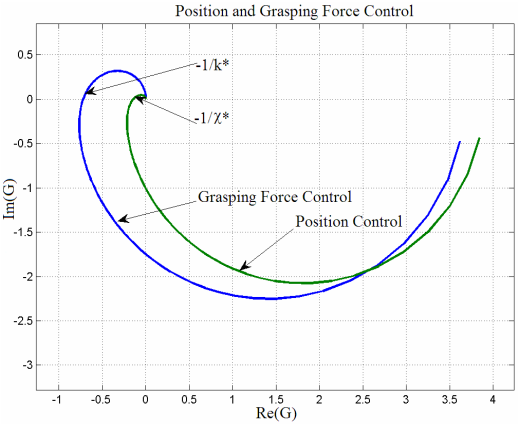

Fig.9. The plot of $G(j\omega)$ for position and force control

Fig.9 shows the frequency plots of $G(j\omega)$ and $\tilde{G}(j\omega)$ for the position and force control, respectively. The plot of $G(j\omega)$ crosses the negative real axis at -0.14, which imposes the limit of tension at $T^* = 7.15N$; the plot of $\tilde{G}(j\omega)$ crosses the negative real axis at -0.74, which corresponds to the critical value of the force sector at $k^* = 1.3$.

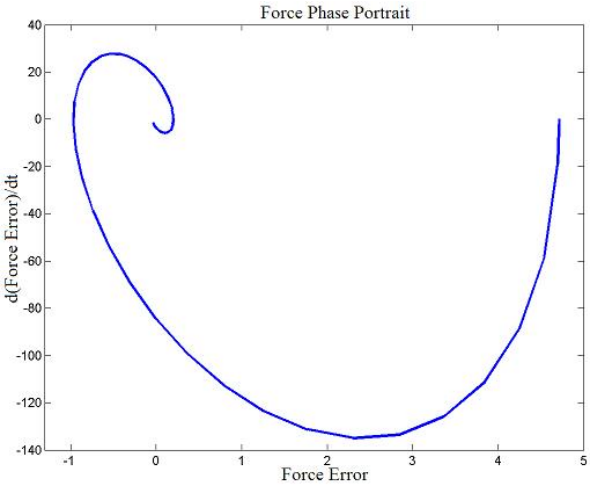

Fig.10. The force phase portrait

A P – control (4.5) with $k_p = 24$ is applied and the force phase portrait is illustrated in Fig.10. Please note the convergence to zero of the force error, but, also, the transient response of the system determined by the P – control law and a low damping factor of the system.

VI. Experimental Results

In order to verify the suitability of the control algorithm, a planar continuum terminal arm consisting by a layer structure has been employed for testing (Fig.11).

The arm consists of two $(25 \times 6 \times 4mm)$ continuum segments with an elastic backbone rod. The two antagonistic SMA actuators ensure the actuation system. Each actuator consists of G fibers in parallel. A polymer thick film layer which exhibits a decrease in resistance with an increase of the film curvature is used. Also, a Force Sensing Resistor is used at the end of each segment.

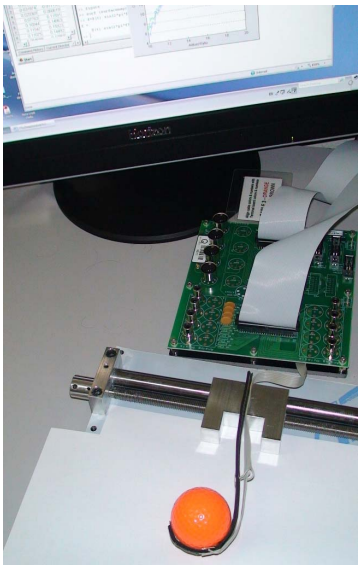

Fig.11. Experimental platform

A Quancer based platform is used for control and signal acquisition. The load is represented by a sphere ball with $R_c = 0.02m$. A P-control with $k_p = 2.17$, $T_D = 5\text{s}$, $T_P = 7\text{s}$ is implemented. The contact force in the grasping operation is represented in Fig.12.

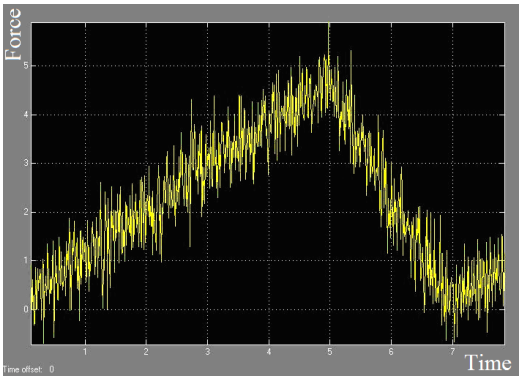

Fig.12. The contact force diagram

VII. Conclusions

The paper treats the control problem of a hyper-redundant robot with continuum elements that performs the coil function for grasping. First, the dynamic model of continuum arm for the position control during non-contact operations with environment is studied and a frequency stability criterion based on KYP Lemma is introduced. The P and PD control algorithms are proposed. Then, the grasping control problem for the arm in contact with a load is analyzed. The dynamics of the system are discussed and an extension of the Popov criterion is proposed. The control algorithms based on SMA actuators are introduced. Numerical simulations and experimental results of the arm motion toward a imposed target prove the correctitude of the solutions.

Appendix 1

Consider the following Lyapunov functional,

$$V = \int_0^L e^T Peds \tag{A.1.1}$$

where P is a (2×2), symmetrical and positive definite matrix. The derivative of this functional will be

$$\dot{V} = \int_0^L \left[\begin{array}{l} \left(\frac{\partial^2 e^T}{\partial s^2} A^T Pe + e^T PA \frac{\partial^2 e}{\partial s^2} \right) + \\ + \left(e^T B^T Pe + e^T PBe \right) + 2e^T Pcf \end{array} \right] ds \tag{A.1.2}$$

By using the relation

$$\frac{\partial^2 e^T}{\partial s^2} A^T Pe = \frac{\partial}{\partial s}\left(\frac{\partial e^T}{\partial s} A^T Pe \right) - \frac{\partial e^T}{\partial s} A^T P \frac{\partial e}{\partial s}, \tag{A.1.3}$$

the derivative $\dot{V}$ will be

$$\begin{aligned} \dot{V} = & \int_0^L \left[\begin{array}{l} -\left(\frac{\partial e^T}{\partial s} \left(A^T P + PA \right) \frac{\partial e}{\partial s} \right) + \\ + e^T \left(B^T P + PB \right) e + 2e^T Pcf \end{array} \right] ds + \\ & + \left(e^T \left(A^T P + PA \right) \frac{\partial e}{\partial s} \right) \Big|_0^L \end{aligned} \tag{A.1.4}$$

By using the inequality [14] and the condition (3) (Theorem 1)

$$\begin{aligned} \int_0^L \frac{\partial e^T}{\partial s} \left(A^T P + PA \right) \frac{\partial e}{\partial s} ds \geq & \int_0^L e^T \left(A^T P + PA \right) eds - \\ & - \left(e^T \left(A^T P + PA \right) e \right) \Big|_0^L \end{aligned}, \tag{A.1.5}$$

$$\begin{aligned} \dot{V} \leq & \int_0^L \left(\begin{array}{l} e^T \left(\left(-A + B \right)^T P + P\left(-A + B \right) \right) e + \\ + 2e^T \left(Pc - \frac{1}{2} n \right) \cdot f + e^T nf \end{array} \right) + \\ & + \left(e^T \left(A^T P + PA \right) \left(e + \frac{\partial e}{\partial s} \right) \right) \Big|_0^L \end{aligned} \tag{A.1.6}$$

If the condition (1) (Theorem 1) is verified and the conditions of the Yakubovich – Kalman – Popov Lemma are met [15]

$$\left(-A + B \right)^T P + P\left(-A + B \right) = -QQ^T \tag{A.1.7}$$

$$Pc - \frac{1}{2} n = \sqrt{k^{-1}} Q \tag{A.1.8}$$

where Q is a vector, k is chosen as $k = \chi$ and $n = \begin{bmatrix} 1, & 0 \end{bmatrix}^T$.

The condition of the frequency domain of the YKP Lemma becomes

$$\frac{1}{\chi} + \mathrm{Re}\left[n^T \left(j\omega I - \left(-A + B \right) \right)^{-1} c \right] \geq 0 \qquad \text{(A.1.9)}$$

Substituting (A.1.7), (A.1.8) in (A.1.6), with the boundary control given by the condition 5 and the boundary conditions (3.15), this inequality becomes

$$\dot{V} \leq -\int_0^L \left(e^T Q - \sqrt{\chi^{-1}} f \right)^2 ds - e_L^T \left(A^T P + PA \right) K e_L \qquad \text{(A.1.10)}$$

where $e_L = \begin{bmatrix} e_\theta(t,L) & e_{\dot{\theta}}(t,L) \end{bmatrix}^T$ and K is a positive definite matrix defined by (4.3).

By using the condition (3) and (5), we can infer that

$$\dot{V} \leq 0 \qquad \text{(Q.E.D.)} \qquad \text{(A.1.11)}$$

APPENDIX 2

Considering the same procedure as in Appendix 1, the boundary conditions (5.3) – (55), and the conditions of the Yakubovich – Kalman – Popov Lemma

$$\left(-\tilde{A} + \tilde{B} \right)^T P + P\left(-\tilde{A} + \tilde{B} \right) = -QQ^T \qquad \text{(A.2.1)}$$

$$P\tilde{c} - \frac{1}{2}\tilde{n} = \sqrt{k_s^{-1}}\, Q \qquad \text{(A.2.2)}$$

where $\tilde{n} = \begin{bmatrix} 1 & 0 & 0 & 0 \end{bmatrix}^T$, and the sector inequality (6.1), (6.3), we obtain

$$\dot{V} \leq \int_0^L \left(-\tilde{e}^T QQ^T e + 2\tilde{e}^T \sqrt{k_s^{-1}}\, Qf - k_s^{-1} f^2 \right) ds + \left(\tilde{e}^T \left(\tilde{A}^T P + P\tilde{A} \right) \left(\tilde{e} + \frac{\partial \tilde{e}}{\partial s} \right) \right) \Bigg|_0^L \qquad \text{(A.2.3)}$$

$$\dot{V} \leq \int_0^L \left(-\tilde{e}Q - \sqrt{k_s^{-1}}\, f \right)^2 - \tilde{e}_L^T \left(\tilde{A}^T P + P\tilde{A} \right) \tilde{K} \tilde{e}_L^T \qquad \text{(A.2.4)}$$

where $\tilde{K}$ is a positive definite matrix and $\tilde{e}_L = \tilde{e}(t,L)$.

Using the boundary conditions (5.1) – (5.5), and the conditions (5) of Theorem 2,

$$\dot{V} \leq 0 \qquad \text{(Q.E.D.)} \qquad \text{(A.2.5)}$$

REFERENCES

[1] Hemami, A., *Design of light weight flexible robot arm*, Robots 8 Conference Proceedings, Detroit, USA, June 1984, pp. 1623-1640.

[2] Gravagne, Ian A., Walker, Ian D., *On the kinematics of remotely - actuated continuum robots*, Proc. 2000 IEEE Int. Conf. on Robotics and Automation, San Francisco, April 2000, pp. 2544-2550.

[3] Gravagne, Ian A., Walker, Ian D., *Kinematic Transformations for Remotely-Actuated Planar Continuum Robots*, Proc. 2000 IEEE Int. Conf. on Rob. and Aut., San Francisco, April 2000, pp. 19-26.

[4] Gravagne, Ian A., Rahn, Christopher D., Walker, Ian D., *Good Vibrations: A Vibration Damping Setpoint Controller for Continuum Robots*, Proc. 2001 IEEE Int. Conf. on Robotics and Automation, May 21-26, 2001, Seoul, Korea, pp. 3877-3884.

[5] Gravagne, Ian A., Walker, Ian D., *Uniform Regulation of a Multi-Section Continuum Manipulator*. Proc. IEEE Int. Conf. on Rob. and Aut, Washington, A1-15, May 2002, pp. 1519-1524.

[6] Chirikjian, G. S., Burdick, J. W., *An obstacle avoidance algorithm for hyper-redundant manipulators*, Proc. IEEE Int. Conf. on Robotics and Automation, Cincinnati, Ohio, May 1990, pp. 625 - 631.

[7] Mochiyama, H., Kobayashi, H., *The shape Jacobian of a manipulator with hyper degrees of freedom,* Proc. 1999 IEEE Int. Conf. on Robotics and Automation, Detroit, May 1999, pp. 2837- 2842.

[8] Robinson, G., Davies, J.B.C., *Continuum robots – a state of the art*, Proc. 1999 IEEE Int. Conf. on Rob and Aut, Detroit, Michigan, May 1999, pp. 2849-2854.

[9] Ivanescu, M., Stoian, V., *A variable structure controller for a tentacle manipulator*, Proc. IEEE Int. Conf. on Robotics and Aut., Nagoya, 1995, pp. 3155-3160.

[10] Ivanescu, M., Florescu, M.C., Popescu, N., Popescu, D., *Position and Force Control of the Grasping Function for a Hyperredundant Arm*, Proc.of IEEE Int. Conf.on Rob. and Aut., Pasadena, California, 2008, pp. 2599-2604.

[11] Camarillo, D., Milne, C., *Mechanics Modeling of Tendon – Driven Continuum Manipulators*, IEEE Trans. On Robotics, vol. 24, no. 6, December 2008, pp. 1262 – 1273.

[12] Wongratanaphisan, T., Cole, M., *Robust Impedance Control of a Flexible Structure Mounted Manipulator Performing Contact Tasks*, IEEE Trans. On Robotics, vol. 25, no. 2, April 2009, pp. 445 – 451.

[13] Grant, D., Hayward, V., *Constrained Force Control of SMA Actuators*, Proc. ICRA 2000, San Francisco, pp. 1314 – 1320.

[14] Mihlin, S. G., *Variationnie Metodi b Matematiceskvi Fizike*, Nauka, Moscva, 1970 (Russian).

[15] Slotine, J.J., Weiping Li, *Applied Nonlinear Control*, Prentice-Hall International Editions, 1991.